

Symmetry-protected collisions between strongly interacting photons

Jeff D. Thompson^{1,2*}, Travis L. Nicholson^{3*}, Qi-Yu Liang³, Sergio H. Cantu³, Aditya V. Venkatramani¹, Soonwon Choi¹, Ilya A. Fedorov⁴, Daniel Viscor⁵, Thomas Pohl^{5†}, Mikhail D. Lukin¹ & Vladan Vuletić³

Realizing robust quantum phenomena in strongly interacting systems is one of the central challenges in modern physical science. Approaches ranging from topological protection to quantum error correction are currently being explored across many different experimental platforms, including electrons in condensed-matter systems¹, trapped atoms² and photons³. Although photon-photon interactions are typically negligible in conventional optical media, strong interactions between individual photons have recently been engineered in several systems^{4–10}. Here, using coherent coupling between light and Rydberg excitations in an ultracold atomic gas, we demonstrate a controlled and coherent exchange collision between two photons that is accompanied by a $\pi/2$ phase shift. The effect is robust in that the value of the phase shift is determined by the interaction symmetry rather than the precise experimental parameters^{7,10–13}, and in that it occurs under conditions where photon absorption is minimal. The measured phase shift of $0.48(3)\pi$ is in excellent agreement with a theoretical model. These observations open a route to realizing robust single-photon switches and all-optical quantum logic gates, and to exploring novel quantum many-body phenomena with strongly interacting photons.

Strong interactions between individual photons can be realized by coupling light to individual atoms^{4,14} or to strongly interacting collective excitations in atomic ensembles¹⁵. In the latter approach, photons are coherently coupled to highly excited Rydberg states in an atomic gas by means of electromagnetically induced transparency (EIT)^{16–18}. The resulting hybrid excitations of light and matter—Rydberg polaritons—inherit strong interactions from their Rydberg components, and can, in principle, propagate with very low photon absorption. Recently, these interactions have enabled the observation of photon blockade^{6,8,9} and bound states of attractive photons¹⁹, as well as the implementation of single-photon transistors^{11–13}. Despite these advances, the realization of controlled, coherent interactions between single photons with low photon absorption, as required for efficient, deterministic, all-optical quantum logic^{7,10}, remains an outstanding experimental challenge.

Our approach to realizing robust, low-loss photon interactions makes use of a collision between stationary and propagating polaritons in a dense atomic gas (Fig. 1a), with the polaritons composed of distinct Rydberg states with opposite parity. This choice of atomic states results in a long-range dipole-dipole interaction^{20–22} between the polaritons. As the polaritons approach each other in the cloud, they coherently switch places under the dipole-dipole interaction, acquiring a phase shift of exactly $\pi/2$ in the process (Fig. 1c). This phase is analogous to that acquired by a spin-1/2 particle undergoing resonant spin rotation. As discussed below, the half-integer value of the phase shift in units of π is protected by the symmetry of the effective Hamiltonian against variations in the experimental parameters, unlike in recent demonstrations of Rydberg-mediated optical nonlinearities^{11–13,19}.

Experimentally, we engineer collisions between polaritons coupled to two Rydberg levels $|S\rangle$ and $|P\rangle$ (Fig. 1b) using a combination of EIT and microwave manipulation between Rydberg states²⁰, in a sequence depicted in Fig. 2a and b. Initially, a single photon from a weak optical ‘gate’ pulse enters the atomic cloud and is slowed and stored in the $|S\rangle \equiv |100S_{1/2}\rangle$ state by switching off the control field in the EIT configuration. A microwave pulse coherently converts the stored, collective $|S\rangle$ excitation to the Rydberg level $|P\rangle \equiv |99P_{3/2}\rangle$. Then, a second ‘signal’

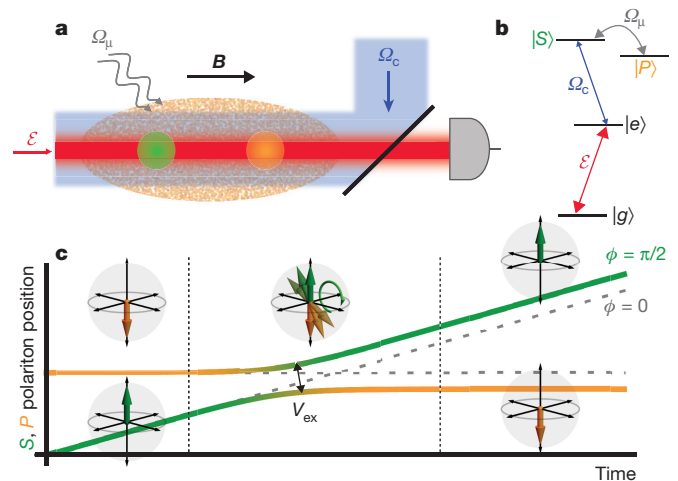


Figure 1 | Photon collisions mediated by long-range exchange

interactions. **a**, Interactions between photons are realized in a gas of laser-cooled ^{87}Rb atoms^{8,19}. Single photons from a weak probe beam (\mathcal{E} , red) are focused to a waist $w_p = 4.5\ \mu\text{m}$, smaller than the transverse cloud dimensions, and coherently coupled to the Rydberg state $|S\rangle \equiv |100S_{1/2}, m_f = 1/2\rangle$ by an intense, counter-propagating control beam with Rabi frequency $\Omega_c/(2\pi) = 16\ \text{MHz}$ (blue) (here, $n = 100$ is the principal quantum number of the Rydberg state and $m_f = 1/2$ is the spin projection along the magnetic field direction). Both beams are circularly polarized, and propagate along the direction of the magnetic field ($B = 0.3\ \text{mT}$). **b**, The probe field at $780\ \text{nm}$ is resonant with the $|g\rangle \equiv |5S_{1/2}, F = 2, m_F = 2\rangle$ to $|e\rangle \equiv |5P_{3/2}, F = 3, m_F = 3\rangle$ transition, where F and m_F indicate the hyperfine and magnetic quantum numbers, respectively. The control field Ω_c at $479\ \text{nm}$ couples $|e\rangle$ to $|S\rangle$. Microwave radiation at $3.7\ \text{GHz}$ with Rabi frequency $\Omega_{\mu}/(2\pi) = 3\ \text{MHz}$ is used to transfer population between Rydberg states, from $|S\rangle$ to $|P\rangle \equiv |99P_{3/2}, m_f = 3/2\rangle$. **c**, A collision is realized between a single, stationary Rydberg excitation in $|P\rangle$ (orange line), and a single, propagating polariton coupled to $|S\rangle$ (green line). As they approach in the cloud, the dipole-dipole interaction V_{ex} causes them to switch places and acquire a phase shift of $\pi/2$. Without interactions, the polaritons pass through each other with no phase acquired (grey dashed lines). The Bloch spheres denote the state of each polariton during the interaction (upwards arrows denote $|S\rangle$; downwards arrows denote $|P\rangle$).

¹Department of Physics, Harvard University, Cambridge, Massachusetts 02138, USA. ²Department of Electrical Engineering, Princeton University, Princeton, New Jersey 08544, USA. ³Department of Physics and Research Laboratory of Electronics, Massachusetts Institute of Technology, Cambridge, Massachusetts 02139, USA. ⁴Russian Quantum Center, Moscow 143025, Russia.

⁵Max Planck Institute for the Physics of Complex Systems, 01187 Dresden, Germany. [†]Present address: Department of Physics and Astronomy, Aarhus University, DK-8000 Aarhus, Denmark.

*These authors contributed equally to this work.

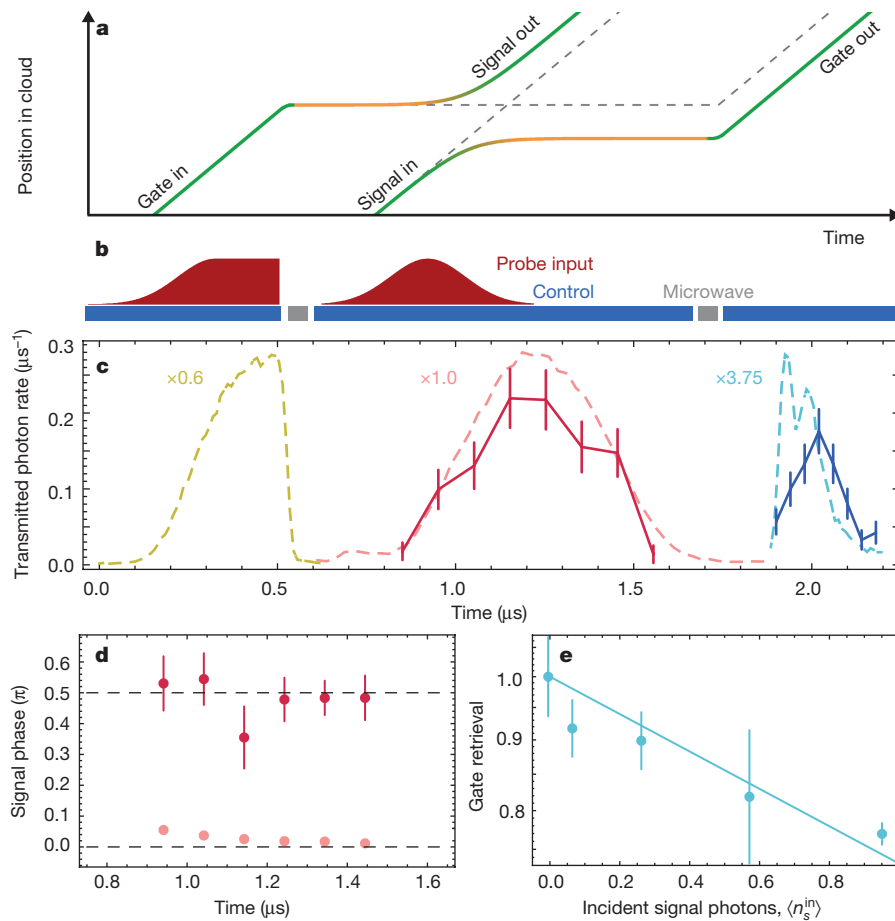


Figure 2 | Observation of photon collisions.

a, b, Illustration of experimental procedure (see text). **c**, Average transmitted intensity through the atomic cloud (dashed lines), showing the leaked gate pulse (yellow, scaled by a factor of 0.6 for display), the signal pulse (red), and the retrieved gate pulse (blue, scaled by a factor of 3.75). The average transmitted intensity is representative of the intensity in the absence of interactions, owing to the low incident photon number. We measure the transmission probability for an incident signal (gate) photon to be 0.56 (0.06) in this case. The dark blue points show the retrieved gate intensity conditioned on the detection of a signal photon in the same experimental cycle, while the dark red points show the transmitted signal intensity conditioned on the detection of a retrieved gate photon. The conditional signal transmission and gate retrieval are 77% and 82% (respectively) relative to their values without interactions. All of the features in the data are quantitatively described by a numerical simulation with independently measured parameters (see Supplementary Information). **d**, Phase of the transmitted signal field with (dark points) and without (light points) conditioning on the detection of a retrieved gate photon. The uniform phase of $\phi_c = 0.48(3)\pi$ in the conditioned case results from the collision with a gate excitation inside the cloud. The phase shift is nearly absent without conditioning ($\phi = 0.03\pi$). **e**, Normalized retrieval efficiency of the stored gate excitation as a function of average signal photon number $\langle n_s^{\text{in}} \rangle$. The data are fitted to an exponential decay of the form $\exp(-\langle n_s^{\text{in}} \rangle / n_d)$, where $n_d^{-1} = 0.26(5)$ is the gate polariton destruction probability per incident signal photon. All displayed error bars represent ± 1 standard deviation.

pulse coupled to the $|S\rangle$ state enters the medium. Since the control laser addresses only $|S\rangle$ (Fig. 1b), the polariton in $|P\rangle$ does not propagate, leading to a collision between the propagating S -state polariton and the stationary excitation in $|P\rangle$. The S -polariton ultimately leaves the cloud and is detected as a photon. Finally, the excitation stored in the $|P\rangle$ state is converted back to a propagating S -polariton (with another microwave pulse) and retrieved. The influence of polariton interactions is observed via the correlations of the transmitted signal and gate photons.

The measured transmitted intensity through the atomic cloud (Fig. 2c) shows the portion of the incident gate pulse that is not stored (henceforth neglected), the transmitted signal pulse, and the retrieved gate pulse. The incoming signal and gate pulses have mean photon numbers less than one ($\langle n_s^{\text{in}} \rangle = 0.25$ and $\langle n_g^{\text{in}} \rangle = 0.15$ for signal and gate, respectively). Therefore, the transmitted intensity averaged over many repetitions of the experiment (dashed lines in Fig. 2c) consists mainly of events with only one of the signal or gate photons present, in which interactions play no role. By examining the retrieved gate conditioned on the detection of a signal photon in the same experimental cycle, we directly observe the polariton interactions, because the gate photons in this case are delayed by an average of approximately 40 ns (corresponding to a 13- μm propagation distance without interactions; solid line in Fig. 2c). We attribute this to the S and P polaritons switching places in the cloud, as shown schematically in Fig. 2a. At the same time, the probability of retrieving the gate photon remains high in the presence of interactions (0.82(7) relative to the non-interacting case). The gate retrieval probability decays exponentially with the number of input signal photons (Fig. 2e), and from the decay constant we extract that the probability for a single signal photon to destroy the stored gate excitation is 0.26(5). This loss is substantially lower than in similar experiments using blockade-type interactions on EIT resonance^{23,24}.

To observe the phase shift resulting from the interaction, we analyse the transmitted signal pulse conditioned on the detection of a

retrieved gate photon. The conditioned phase of the transmitted signal (measured by interference with a co-propagating, far-detuned local oscillator) is $\phi_c = 0.48(3)\pi$ (Fig. 2d). Without conditioning, the signal phase $\phi = 0.03\pi$; this difference confirms that the phase arises from interaction with a single gate excitation ($\phi = 0$ is defined by a control experiment with $n_g^{\text{in}} = 0$). At the same time, the signal transmission is only reduced by a factor of 0.77(6) compared to its value without interactions (Fig. 2c). The high transmission, together with the uniformity of the $\pi/2$ phase shift across the pulse, establishes that polariton collisions under dipolar interactions are highly coherent.

To demonstrate the robustness of the phase shift, we repeated the measurements in Fig. 2c and d for a range of atomic densities, as summarized in Fig. 3. For each density, we measure the conditioned phase shift ϕ_c of the transmitted signal field, as well as the joint probability T_c of both signal and gate photons being transmitted, relative to their independent transmission probabilities. The phase shift saturates at $\phi_c = \pi/2$ at high densities, indicating that it is a robust property of the photon collision. The transmission probability has a minimum at intermediate densities and it improves in the high-density limit, in stark contrast to conventional resonant dipole blockade, where transmission is exponentially suppressed at high densities⁸.

The emergence of the phase shift can be understood from a simple model incorporating propagation and interactions. Letting $\psi(r, r')$ denote the two-body spatial wavefunction for polaritons at positions r and r' coupled to states $|S\rangle$ and $|P\rangle$, respectively, we show in the Supplementary Information that the evolution of the system (in the limit of large atomic density) is governed by the effective Schrödinger equation:

$$i \frac{\partial}{\partial t} \psi(r, r') = -i v_g \frac{\partial}{\partial r} \psi(r, r') + \frac{1}{\hbar} V_{\text{ex}}(r - r') \psi(r', r) \quad (1)$$

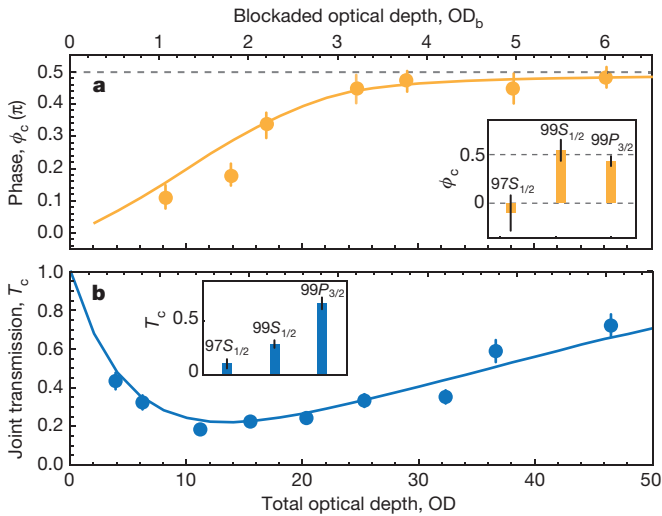


Figure 3 | Density dependence and robustness of the scattering phase. **a**, Conditioned phase shift ϕ_c over a range of atomic densities, quantified by the total optical depth, OD. Also shown on the top axis is the estimated optical depth over one blockade radius r_b , for a Rydberg excitation at the centre of the cloud (OD_b , see text). **b**, Joint probability of the signal and gate photons being transmitted, relative to their independent transmission without interactions: $T_c = \langle n_s n_g \rangle / (\langle \tilde{n}_s \rangle \langle \tilde{n}_g \rangle)$. Here, \tilde{n}_s (\tilde{n}_g) denotes the number of detected signal (gate) photons in a control measurement with $n_g^{\text{in}} = 0$ ($n_s^{\text{in}} = 0$), while n_s and n_g are the number of detected photons for average input photon numbers, $\langle n_s^{\text{in}} \rangle = 0.25$ and $\langle n_g^{\text{in}} \rangle = 0.15$. The lines show the result of a numerical simulation of the storage, interaction and retrieval stages of the experiment, including experimental non-idealities such as dephasing from Rydberg-ground-state collisions (see Supplementary Information). The insets show the results of similar experiments at high optical depths (OD = 55), with the state $|P\rangle$ replaced by $|97S_{1/2}\rangle$ or $|99S_{1/2}\rangle$. These have weaker or absent dipole-dipole interactions with $|S\rangle$ (see text).

where v_g denotes the S-polariton group velocity, and $V_{\text{ex}}(r-r') = C_3/|r-r'|^3$ is the dipolar interaction between the states $|S\rangle$ and $|P\rangle$, whose action on the polaritons at r and r' is to swap their positions, coupling the state $\psi(r, r')$ to $\psi(r', r)$. Equation (1) has a simple time-independent solution in the continuous-wave limit:

$$\psi(r, r') = \exp[-r_s^2/2(r-r')^2] \exp\{-i \text{sgn}[(r-r')C_3] \pi/4\}$$

Here, $r_s = \sqrt{C_3/(v_g \hbar)}$ is the ‘hopping radius’, which is the distance at which the approaching polaritons exchange their positions and start propagating away from each other. Correspondingly, there is very little probability of finding the polaritons at distances $|r-r'| < r_s$. The complex transmission coefficient:

$$t_c = \frac{\lim_{(r-r') \rightarrow \infty} \psi(r, r')}{\lim_{(r-r') \rightarrow -\infty} \psi(r, r')}$$

takes the value $e^{\pm i\pi/2}$, depending on the sign of C_3 .

Remarkably, this robust phase shift can be understood by considering the symmetries of the effective Hamiltonian H_{eff} governing equation (1). In the centre-of-mass frame, $\mathbb{P}H_{\text{eff}} = -H_{\text{eff}}\mathbb{P}$, under the transformation $\mathbb{P}: \psi(r, r') \mapsto \text{sgn}(r'-r)\psi^*(r, r')$. \mathbb{P} is analogous to the particle-hole symmetry encountered in fermionic condensed matter systems^{25,26}, and constrains the structure of the eigenstates of H_{eff} such that t_c must be purely imaginary for low-energy scattering processes, ensuring a phase shift of $\pm\pi/2$ regardless of the precise parameters in equation (1) (see Supplementary Information for a detailed discussion).

The model in equation (1) does not include absorption from interaction-induced level shifts, which may occur when $V_{\text{ex}}(r-r')$ exceeds the linewidth of the EIT transparency window γ_{EIT} (ref. 17). Absorption will

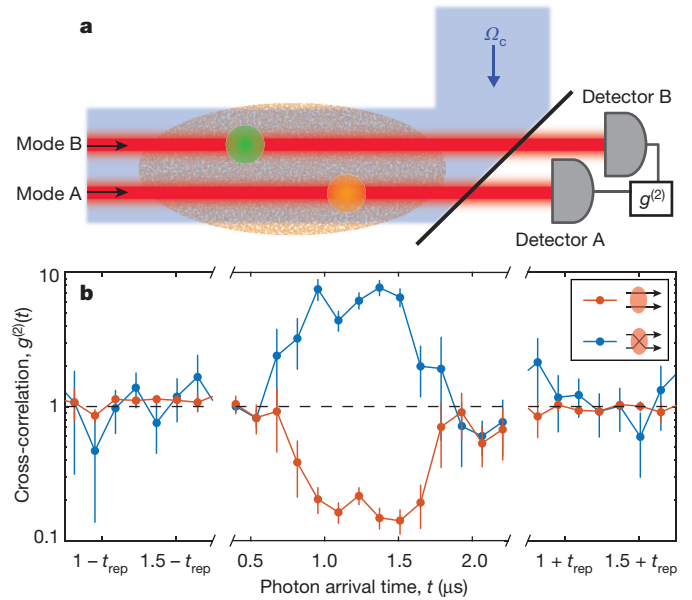


Figure 4 | Polariton exchange between separated transverse modes. **a**, The gate and signal pulses are now incident in distinct transverse spatial modes, A and B, respectively, separated by $1.2w_p = 5.4\mu\text{m}$. The control beam addresses both modes. **b**, The intensity cross-correlation between signal and gate photons exiting in their incident modes (red points, $g_{\text{inc}}^{(2)}$) and in swapped modes (blue points, $g_{\text{sw}}^{(2)}$) shows that polaritons switch modes in the cloud. $g_{\text{inc}}^{(2)}(t) = \langle n_s^B(t)n_g^A \rangle / (\langle n_s^B(t) \rangle \langle n_g^A \rangle)$, where $n_s^B(t)$ denotes the number of signal photons detected at time t in mode B, and n_g^A is the total number of gate photons detected in mode A. The definition for $g_{\text{sw}}^{(2)}(t)$ is the same, with the modes A and B reversed. The correlations are absent for photons separated by the repetition time of the pulse sequence, t_{rep} .

occur when polaritons are within the so-called blockade radius, $r_b = (2C_3/\gamma_{\text{EIT}})^{1/3}$. The blockade radius is related to the hopping radius by $r_s = \sqrt{OD_b/2}r_b$. Here, OD_b is the optical depth over a distance r_b , which is proportional to the atomic density. Importantly, if $OD_b > 2$, then $r_s > r_b$, which allows the exchange interaction to take place before the polaritons are sufficiently close to experience absorption. Experimentally, the minimum transmission measured in Fig. 3b occurs at $OD_b \approx 2$, beyond which the transmission indeed steadily increases. This analysis validates the use of equation (1) in the high-density limit $OD_b \gg 1$. A more detailed calculation (see Supplementary Information) shows that the photon loss decreases asymptotically as $OD_b^{-3/2}$ while the phase difference from $\pi/2$ decreases as e^{-OD_b} . This scaling is more favourable than that corresponding to off-resonant Rydberg blockade, where the loss under optimized conditions decreases as OD_b^{-1} (refs 13 and 17).

To further verify the interaction mechanism, we repeated the experiment with other pairs of Rydberg states (Fig. 3 insets) that exhibit different interactions. In contrast to the interaction between $|P\rangle = |99P_{3/2}\rangle$ and $|S\rangle$, which is almost purely dipolar (resulting in a much stronger exchange interaction than the blockade), $|97S_{1/2}\rangle$ interacts with $|S\rangle$ almost entirely through a level-shifting van der Waals process (see Supplementary Information). This results in very low transmission, in agreement with recent photon transistor experiments^{11,12}. The state $|99S_{1/2}\rangle$ has comparable van der Waals and (second-order) dipolar interactions with $|S\rangle$, and shows moderately high transmission and a large phase shift. Since the van der Waals interaction breaks the symmetry protecting the $\pi/2$ phase shift, its value is not robustly $\pi/2$, and will depend on a variety of experimental parameters, including the atomic density and the control field Rabi frequency Ω_c .

Finally, in Fig. 4, we demonstrate that the long-range nature of the interaction allows photons to hop between separated transverse optical

modes. We repeat the experimental sequence in Fig. 2a, but with the gate and signal fields incident in distinct transverse spatial modes (Fig. 4a). Intensity cross-correlation measurements between the transmitted light in the two modes (Fig. 4b) reveal anti-correlations between signal and gate photons exiting in their incident modes ($g_{\text{inc}}^{(2)} = 0.18$) and positive correlations between signal and gate photons exiting in swapped modes ($g_{\text{sw}}^{(2)} = 5.8$). Together, these show that the interaction causes pairs of photons to hop between modes in the atomic cloud, such that the signal exits in the mode in which the gate was incident, and vice versa. By comparison to a control measurement without interactions, we estimate an 8% probability for photons to swap modes due to the exchange process (see Supplementary Information). Compared to the analogous quantity $T_c = 0.77$ measured for single-mode interactions in Fig. 3, this value is lower because of the increased distance between the photons, lower atomic density in the wings of the cloud, and nonlinear effects resulting from higher input power.

The overall efficiency is mostly determined by the finite signal transmission (0.56, limited by laser linewidth) and finite retrieval probability for the gate photon (0.06, limited by imperfect storage and dephasing of the spin wave) in the absence of interactions. These probabilities can be increased to greater than 0.9 with realistic technical improvements: improved laser stability, larger optical depth, better cooling and an optimal choice of Rydberg states (see Supplementary Information). The losses associated with the interaction (resulting in an additional 20% reduction of the two-photon transmission) can be suppressed by increasing OD_{b} , as in Fig. 3b. Because the phase shift is protected against these imperfections by symmetry, higher-fidelity quantum logic may be achieved probabilistically by heralding on the detection of the final transmitted photons.

Our results open up new possibilities for realizing robust quantum gates and many-body phenomena with strongly interacting photons. A modest extension of this work should allow for a controlled π phase shift quantum gate between two photons⁷, by using microwave control to pass the polaritons through each other a second time before they exit the cloud. The demonstrated interaction between polaritons is also a powerful tool for studying the quantum many-body dynamics of photons. In particular, the symmetries that result in the robust phase shifts observed in this work are identical to those that result in Majorana fermions in one-dimensional wires^{27,28}, which are expected to feature similarly robust $\pi/2$ phase shifts under braiding operations¹. Although the present two-particle scattering process has important distinctions, in that the low-energy mode is not protected by an energy gap, the latter could potentially be engineered (for example, via polariton interactions). Likewise, extensions along the lines of recent proposals^{29,30} could be explored to realize topological photonic systems.

Data Availability Data are available from the authors upon request.

Received 16 August; accepted 7 November 2016.

Published online 25 January 2017.

1. Stern, A. & Lindner, N. H. Topological quantum computation—from basic concepts to first experiments. *Science* **339**, 1179–1184 (2013).
2. Monroe, C. & Kim, J. Scaling the ion trap quantum processor. *Science* **339**, 1164–1169 (2013).
3. Lu, L., Joannopoulos, J. D. & Soljačić, M. Topological photonics. *Nat. Photon.* **8**, 821–829 (2014).
4. Birnbaum, K. *et al.* Photon blockade in an optical cavity with one trapped atom. *Nature* **436**, 87–90 (2005).
5. Chang, D. E., Vuletić, V. & Lukin, M. D. Quantum nonlinear optics — photon by photon. *Nat. Photon.* **8**, 685–694 (2014).
6. Dudin, Y. O. & Kuzmich, A. Strongly interacting Rydberg excitations of a cold atomic gas. *Science* **336**, 887–889 (2012).

7. Hacker, B., Welte, S., Rempe, G. & Ritter, S. A photon–photon quantum gate based on a single atom in an optical resonator. *Nature* **536**, 193–196 (2016).
8. Peyronel, T. *et al.* Quantum nonlinear optics with single photons enabled by strongly interacting atoms. *Nature* **488**, 57–60 (2012).
9. Pritchard, J. D. *et al.* Cooperative atom–light interaction in a blocked Rydberg ensemble. *Phys. Rev. Lett.* **105**, 193603 (2010).
10. Beck, K., Hosseini, M., Duan, Y. & Vuletić, V. Large conditional single-photon cross-phase modulation. *Proc. Natl Acad. Sci. USA* **113**, 9740–9744 (2016).
11. Gorniaczyk, H., Tresp, C., Schmidt, J., Fedder, H. & Hofferberth, S. Single photon transistor mediated by Rydberg interaction. *Phys. Rev. Lett.* **113**, 053601 (2014).
12. Tiarks, D., Baur, S., Schneider, K., Durr, S. & Rempe, G. Single-photon transistor using a Förster resonance. *Phys. Rev. Lett.* **113**, 053602 (2014).
13. Tiarks, D., Schmidt, S., Rempe, G. & Dürr, S. Optical π phase shift created with a single-photon pulse. *Sci. Adv.* **2**, e1600036 (2016).
14. Schuster, I. *et al.* Nonlinear spectroscopy of photons bound to one atom. *Nat. Phys.* **4**, 382–385 (2008).
15. Lukin, M. *et al.* Dipole blockade and quantum information processing in mesoscopic atomic ensembles. *Phys. Rev. Lett.* **87**, 037901 (2001).
16. Friedler, I., Petrosyan, D., Fleischhauer, M. & Kurizki, G. Long-range interactions and entanglement of slow single-photon pulses. *Phys. Rev. A* **72**, 043803 (2005).
17. Gorshkov, A. V., Otterbach, J., Fleischhauer, M., Pohl, T. & Lukin, M. D. Photon–photon interactions via Rydberg blockade. *Phys. Rev. Lett.* **107**, 133602 (2011).
18. Petrosyan, D., Otterbach, J. & Fleischhauer, M. Electromagnetically induced transparency with Rydberg atoms. *Phys. Rev. Lett.* **107**, 213601 (2011).
19. Firstenberg, O. *et al.* Attractive photons in a quantum nonlinear medium. *Nature* **502**, 71–75 (2013).
20. Maxwell, D. *et al.* Storage and control of optical photons using Rydberg polaritons. *Phys. Rev. Lett.* **110**, 103001 (2013).
21. Ravets, S. *et al.* Coherent dipole–dipole coupling between two single Rydberg atoms at an electrically-tuned Förster resonance. *Nat. Phys.* **10**, 914–917 (2014).
22. Saffman, M., Walker, T. G. & Molmer, K. Quantum information with Rydberg atoms. *Rev. Mod. Phys.* **82**, 2313–2363 (2010).
23. Gorniaczyk, H. *et al.* Enhancement of Rydberg-mediated single-photon nonlinearities by electrically tuned Förster resonances. *Nat. Commun.* **7**, 12480 (2016).
24. Murray, C. R., Gorshkov, A. V. & Pohl, T. Many-body decoherence dynamics and optimized operation of a single-photon switch. *New J. Phys.* **18**, 092001 (2016).
25. Beenakker, C. W. J. Random-matrix theory of Majorana fermions and topological superconductors. *Rev. Mod. Phys.* **87**, 1037–1066 (2015).
26. Schnyder, A. P., Ryu, S., Furusaki, A. & Ludwig, A. W. W. Classification of topological insulators and superconductors in three spatial dimensions. *Phys. Rev. B* **78**, 195125 (2008).
27. Kitaev, A. Y. Unpaired Majorana fermions in quantum wires. *Phys. Uspekhi* **44** (Suppl.), 131–136 (2001).
28. Mourik, V. *et al.* Signatures of Majorana fermions in hybrid superconductor–semiconductor nanowire devices. *Science* **336**, 1003–1007 (2012).
29. Maghrebi, M. F. *et al.* Fractional quantum Hall states of Rydberg polaritons. *Phys. Rev. A* **91**, 033838 (2015).
30. Sommer, A., Büchler, H. P. & Simon, J. Quantum crystals and Laughlin droplets of cavity Rydberg polaritons. Preprint at <https://arxiv.org/abs/1506.00341> (2015).

Supplementary Information is available in the online version of the paper.

Acknowledgements We acknowledge conversations with A. V. Gorshkov, M. J. Gullans, O. Firstenberg, S. Hofferberth and R. Johne. Funding was provided by the NSF, the Center for Ultracold Atoms, DARPA, ARO, ARO MURI, AFOSR MURI, the ARL, U-FET grant number 512862 (HAIRS), the H2020-FETPROACT-2014 grant number 640378 (RYSQ), the DFG (SPP 1929) and the Kwanjeong Educational Foundation.

Author Contributions The experiment and analysis were carried out by J.D.T., T.L.N., Q.-Y.L., S.H.C., A.V.V. and I.A.F. Theoretical modelling was done by S.C., D.V. and T.P. All work was supervised by M.D.L. and V.V. All authors discussed the results and contributed to the manuscript.

Author Information Reprints and permissions information is available at www.nature.com/reprints. The authors declare no competing financial interests. Readers are welcome to comment on the online version of the paper. Correspondence and requests for materials should be addressed to M.D.L. (lukin@physics.harvard.edu) or V.V. (vuletic@mit.edu).

Reviewer Information *Nature* thanks M. Saffman and the other anonymous reviewer(s) for their contribution to the peer review of this work.